

Self-consistent-field theory of a brush of randomly branched polymers

Shi-Min Cui

Department of Physics, University of Waterloo, Waterloo, Ontario, Canada N2L 3G1

Zheng Yu Chen

Guelph-Waterloo Program for Graduate Work in Physics and Department of Physics, University of Waterloo, Waterloo, Ontario, Canada N2L 3G1

(Received 10 June 1996; revised manuscript received 29 July 1996)

The conformational properties of randomly branched polymers grafted at one end on a planar surface in the good solvent regime are investigated by using a Flory-type scaling theory and by solving a self-consistent-field model numerically. The average monomer height obtained from the self-consistent-field model is shown to be in agreement with the scaling behavior predicted from the scaling theory. The density profile is found to have a near-parabolic form with some discrepancies near the surface and the brush end. [S1063-651X(97)05501-3]

PACS number(s): 36.20.-r, 82.65.Dp, 61.25.Hq

I. INTRODUCTION

The study of the behavior of tethered polymer chains has attracted considerable interest due to the wide range of practical applications [1]. Several approaches, including scaling analyses [2,3], self-consistent-field theories [4–10], and Monte Carlo (MC) [11–14] and molecular-dynamics simulations [15,16], have been employed to model these systems. In these studies, the conformational properties of linear polymer brushes are consistently shown to obey universal scaling laws. Branched polymers, naturally occurring or chemically synthesized, are also expected to display various static and dynamic scaling behaviors that are system independent. It is a challenging and certainly not a trivial theoretical problem to understand the conformational properties of the polymer brush formed by branched polymers. Recently, Carignano and Szleifer [17] explored the conformational and thermodynamic properties of grafted Y-shaped polymer brushes by using an approach based on the probability distribution function formalism [10]. Zhulina and Vilgis [18] presented a simple scaling analysis for the brushes formed by regularly and randomly branched polymers.

While many statistical properties of regularly branched polymers such as comb, star, and starburst polymers are similar, *randomly* branched polymers (RBPs) form their own classes of properties that are, in general, quite different from those of the regular ones. In the present work, we study scaling behaviors of the brush height and monomer density of a brush formed by randomly branched polymers in a good solvent with one end grafted to a planar surface. According to the classification of Gutin, Grosberg, and Shakhnovich [19], RBPs should be further distinguished according to their branching structures. Those with *annealed* branchings and those with *quenched* branchings may display different behaviors. In this paper we focus on the properties of annealed branched polymers, whose branching structures are controlled by maintaining a constant branching activity and thus are directly affected by the monomer-monomer interactions. This implies that there is an additional, structural entropic contribution to the free energy besides a conventional, con-

formational entropic contribution [19]. We present below a Flory-type argument that includes these entropic contributions and an excluded-volume energy, which leads to a power-law scaling behavior of the average brush height as a function of the molecular weight and surface coverage. The resulting “brush exponent” to be defined below, is different from that of quenched RBP brushes recently studied by Zhulina and Vilgis [18].

We have also performed a numerical calculation based on the self-consistent-field (SCF) approximation to further support our conclusion. As is well known, the SCF approximation is a powerful method to treat confined systems consisting of many interacting polymers [4]. The basic technique is to obtain the information on chain configurations represented by the end-to-end Green’s function by solving a partial equation subject to a potential that, in turn, depends on the monomer density self-consistently. For linear brushes, the analytical SCF theory [7,8] yields a simple analytic prediction for the structure of the system of moderately high surface coverage. For instance, the segment density profile and the potential field are found to be parabolic, of the form $a - bz^2$, where z is the distance from the surface. For RBP brushes, the SCF model [20] allows us to examine the basic structure of the theory, but is almost impossible to be solved analytically. We thus resort to a numerical SCF method for the investigation. Our method is based on the statistics of a single polymer brush and overcomes the usual difficulties associated with modeling many polymers simultaneously in a typical computer simulation. For linear polymer brushes, this method generates results in overall agreement with the analytical SCF theory.

This paper is organized as follows. A Flory-type argument for the height of the brush is presented in Sec. II, while a scaling theory based on the blob assumption is discussed in the Appendix. A mean-field theory for the systems of interacting randomly branched polymers is briefly discussed and a MC numerical method is proposed in Sec. III. The results for a variety of molecular weights and surface coverages of linear-chain and annealed RBP brushes are presented in Sec. IV. Section V is devoted to a summary.

II. SCALING ANALYSIS

The Flory-type argument is a simple and efficient theoretical treatment for the scaling behaviors in many polymer systems. When it is applied to linear-polymer brushes in good solvents, the conformational properties are determined by balancing the repulsive excluded-volume interaction energy with the entropic energy penalty of stretching a typical chain away from the grafting surface. The scaling form for the average height is obtained by minimizing the free energy with respect to h , which yields $h \sim N(u\sigma)^{1/3}$, where h is the brush height, N the molecular weight of a single chain, σ the number of chains per unit surface area, and u the excluded-volume parameter of two interacting monomers [2]. For moderate σ and large N , this result agrees with those obtained by other methods, such as the scaling argument [3] that is based on a blob model, the analytical SCF theory [7,8] that utilizes a classical trajectory approach, and numerical simulations [13,14] that are based on various numerical methods.

We consider a RBP brush grafted at one end on a planar surface with a grafting coverage σ in a good solvent. Each monomer, except the one directly embedded on the surface, is assumed to be trifunctional, from which a branch may grow with a certain branching probability Λ^2 . According to Gutin, Grosberg, and Shakhnovich [19], the Flory-type free energy for such a polymer, moving freely in a solvent, contains three terms F_e , F_r , and F_s corresponding to the elastic energy, the volume interaction potential, and the entropy contribution from the rearrangement of branching structures, respectively. The elastic energy has the form

$$F_e = \frac{h^2}{L}, \quad (1)$$

where L is the average contour length of a representative branch starting at the surface grafting site to a free external end. The energy of the excluded-volume interaction between a representative polymer with the mean-field density $\sigma N/h$ produced by the monomers is approximated by

$$F_i = u\sigma \frac{N^2}{h}. \quad (2)$$

The excluded-volume interaction is responsible not only for making polymers stretching away from the surface but also affects the statistics of the branching structure. The conformation entropic contribution to the energy due to such an effect can be evaluated [19,21] by using de Gennes' diagrammatic method [22]

$$F_s = \frac{L^2}{N/\Lambda}. \quad (3)$$

In comparing with Gutin, Grosberg, and Shakhnovich's original expression [19], we have introduced the factor Λ in Eq. (3) in order to account for the branching probability, which is assumed to be related to the mean tribranching number n_3 of the molecules [22,23]

$$\Lambda = \frac{n_3}{N}, \quad (4)$$

when the large- N limit is considered. de Gennes showed Eq. (4) in Ref. [22] for RBP solutions in the θ point condition. We showed earlier [23] through perturbation expansion that in the case of annealed RBPs in a good solvent, the same relation is valid asymptotically for large N . Caution should be used in the practical use of Eq. (4), as n_3/N may vary dramatically at small N and n_3 , and approaches an N -independent constant only at large N . In this paper, we assume without proof that the same relation exists even in the case of imposing a hard-wall boundary condition.

Minimizing the free energy $F = F_e + F_i + F_s$ with respect to L and h we find the expression for the equilibrium brush height

$$h \sim (u\sigma)^{3/7} N \Lambda^{-1/7}. \quad (5)$$

We may rewrite this equation in terms of the ratio h/h_0 where $h_0 \sim l(N/\Lambda)^{1/4}$ [24] is the mean brush height of ideal polymers when no interaction is present

$$\frac{h}{h_0} \approx \Omega^\lambda, \quad (6)$$

where

$$\Omega = u\sigma\Lambda^2 \left(\frac{N}{\Lambda}\right)^{7/4}. \quad (7)$$

The brush exponent $\lambda(\text{Flory}) = \frac{3}{7}$ characterizes the scaling behavior of RBP brushes.

The Flory-type theory presented above is valid in the density regime where the approximation of the second virial coefficient can be adopted for the interaction energy. The particular form of the interaction energy in Eq. (2) explicitly reflects this approximation. Polymer brushes of high-volume density behave more like a polymer melt, which cannot be described simply by the quadratic term in the density. Higher-order virial coefficients must be included. The Flory-Huggins energy $(1-\phi)\ln(1-\phi)$, where ϕ is the volume fraction, is probably a more suitable choice for qualitatively describing the high-volume-density behavior. Another potential problem of the Flory-type theory is its use of the elastic energy of the form in Eq. (1), which is based on a Gaussian-like distribution function for h . Since the distribution function could be quite different from the Gaussian form at the highly stretched limit, the elastic energy that acts to confine the polymers near the surface is underestimated at this limit. Generally, the Flory-type theory and the scaling behavior predicted from it are valid in the moderate-volume-density regime.

An interesting similarity exists between the expressions for the mean brush heights of randomly branched polymers and linear polymers: both depend linearly on N . The fact that RBPs with annealed branchings may attempt to move the branching points farther from the surface to acquire more packing space makes the density distribution function quite smooth, if not flat. We may use the linear dependence on N as the starting point for a scaling theory based on the blob model similar to that proposed by de Gennes [2] for the linear brushes. As shown in the Appendix, such a theory results in the same scaling behavior predicted by the Flory-type theory presented above.

Zhulina and Vilgis [18], however, studied the brush formed by attaching one end of branched polymers with *quenched* branching structures to a flat surface. It has been generally shown that annealed and quenched randomly branched polymers behave differently in a good solvent [19,21]. The theory of Zhulina and Vilgis [18] is equivalent to using the free energy $F = F_e + F_r$ with the mean length L in Eq. (1) replaced by its mean value at the θ temperature h_0^2 . The third term in the free energy Eq. (3) does not exist due to the fixed topology. The resulting equilibrium mean height also has the scaling form given by Eqs. (6) and (7), however, with a different brush exponent $\lambda'(\text{Flory}) = \frac{1}{3}$. In terms of a direct power-law expression, $h(\text{quenched}) = (u\sigma)^{1/3} N^{5/6} \Lambda^{-1/6}$. The major difference between the annealed and quenched cases is in the scaling dependence on N : annealed polymers tend to stretch farther from the surface and the quenched polymers tend to maintain a “slower” power-law behavior because of the structure constraint. The structure constraint further sets a maximum extension limit on the quenched polymers [18], while the annealed polymers can, in principle, be rearranged and stretched to reach a maximum extension of Nl from the surface, with the cost of losing conformational and structural entropies. It is worth noting that the brush exponent for quenched RBP brushes ($\lambda = \frac{1}{3}$) is the same as the exponent that governs the scaling behavior of linear-chain brushes, when the latter is expressed in terms of scaled variables in a form similar to Eq. (6).

III. SELF-CONSISTENT-FIELD MONTE CARLO METHOD

An elegant result in the theory of linear polymer brushes is the parabolic solution of the density profile derived by Milner, Witten, and Cates [7] and Skvortsov *et al.* [8]. This analytic result sets an asymptote for the $N \gg 1$ limit and has been checked by various numerical simulations. The success of the theory largely depends on the similarity in the formulation structures of the linear polymer theory and the classical dynamics of a single particle.

The mean-field theory for branched polymers, however, lacks its analogy in classical mechanics. The important physical quantity is the Green's function $G_0(\mathbf{r}, \mathbf{r}'; t)$ of a randomly branched polymer containing t monomers with two external ends having positions denoted by vectors \mathbf{r} and \mathbf{r}' , which can be shown [20] to obey a nonlinear partial differential equation in the presence of a mean field. For RBP brushes grafted on a flat surface, the mean field can be considered as a function of the variable z along the normal to the surface,

$$\omega(z) = u\rho(z), \quad (8)$$

where u is the excluded-volume parameter and $\rho(z)$ is the average monomer density. By summing over the probability of configurations passing through a spatial point z , $\rho(z)$ is determined by the three-point correlation function [23], which satisfies a complicated equation due to the branching structures [see Eq. (3.2) of [23]]. Note that $\rho(z)$ is directly proportional to the number of polymers per unit grafting-surface area σ in the SCF approximation and thus that u and σ appear as a single combination.

There are several numerical procedures in the literature to solve the mean-field equation for linear polymer systems

[4–6,9,10]. However, it is very difficult to generalize these methods to obtain the monomer density of the RBP systems by solving the SCF equations [20]. Here we adopt a MC numerical procedure that enables us to calculate the density profile directly by using Eq. (8). The main idea is to isolate the structure complicity, which is modeled by a MC procedure, from making a mean-field approximation for the interaction energy.

We used an iterative MC simulation method, which contains the following procedure. An initial density profile $\rho(z)$ was proposed and used in the mean potential field $\omega(z) = u\rho(z)$ for an initial MC run, in which the statistics of polymers with different branching structures and configurations were sampled and a new average density profile was “measured.” This profile was then used as an approximation for the mean field of the next run and a new density profile was produced. The procedure was considered convergent when the relative difference between density profiles of the two consecutive runs became smaller than a preset criterion. This method was shown to be very efficient for solving the grafted problems of linear chains as well as randomly branched polymers.

More specifically, each MC run consisted of a number of MC steps. The MC method used in this study is a generalization of the off-lattice pivot method developed for the homogeneous systems of randomly branched polymers [21], except for the part of imposing a hard-bead interaction, which is now represented by the effective mean field. In our simulations, the RBP model was treated as a treelike molecule of links of N identical rigid bonds of length l , freely jointed together in three-dimensional space, with one end permanently fixed at $\mathbf{r} = \mathbf{0}$. The flat surface was assumed impenetrable and placed parallel to the x - y plane at $z = 0$. The other monomers were constrained to move in the positive half space ($z > 0$). For a flat surface, we broke the space into discrete slabs of width $l/4$ and treated the density within each slab as a constant. The density was then calculated as a function of z only, due to the symmetry; no x or y dependence was taken into consideration. At every MC step, a branching position was chosen at random and one of the neighboring bonds was cut to produce two pieces of the polymer: one still connected to the surface and another free from the surface. The free portion of the polymer was rotated as a rigid body to a new position randomly. Then an arbitrary point on the unrotated portion of the polymer was located for reconnecting the two pieces. The configuration was rejected if the chosen point was already branched. Each monomer was subject to an external potential $u\rho(z)$. Subsequently, the new configuration was accepted or rejected according to the usual Metropolis algorithm of comparing the Boltzmann factors corresponding to the two configurations. At this point we calculated the average monomer distribution function. A typical run consisted of approximately $2N \times 10^4$ MC steps.

In the next run, the obtained density profile was substituted into the mean field and a new density profile was calculated the same way. The moments of the density profile

$$\langle z^n \rangle \equiv \int_0^\infty z^n \rho(z) dz / \int_0^\infty \rho(z) dz \quad (n = 1, 2, \dots) \quad (9)$$

were calculated at the end of each run. The iterations of a

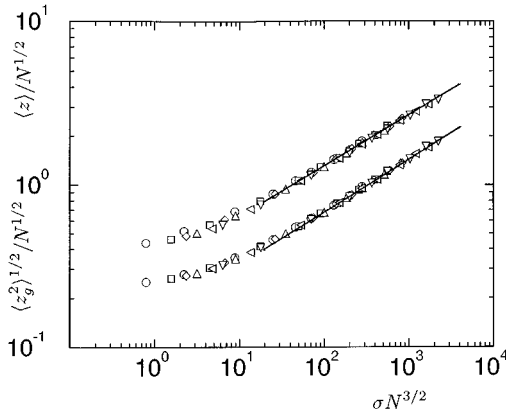


FIG. 1. Scaled average brush height $\langle z \rangle / N^{1/2}$ and the mean-square radius of gyration normal to the surface $\langle z_g^2 \rangle^{1/2} / N^{1/2}$ of a linear brush plotted as a function of $\sigma N^{3/2}$ on a log-log scale for $\sigma = 0.025$ (circles), 0.05 (squares), 0.075 (diamonds), 0.10 (up triangles), 0.15 (left triangles), and 0.20 (down triangles). The two straight lines indicate the asymptotic behavior with the same slope of $\frac{1}{3}$.

series of runs were terminated when the relative difference between the new and old moments $\langle z^n \rangle$ ($n=1,2,\dots,10$) of the density profiles became less than 10^{-3} . For a given set of molecular weight and surface coverage, a typical calculation that was performed contained usually less than four iterations.

IV. RESULTS AND DISCUSSION

The algorithm proposed above is quite general and is independent of the type of polymers under study. To test our algorithm, we first studied *linear* polymer brushes for various surface coverages $\sigma = 0.025, 0.05, 0.075, 0.10, 0.15, 0.20$ and various chain lengths $N = 10, 20, 50, 100, 150, 200, 300, 400, 500$. The average monomer height and the root-mean-square radius of gyration $\langle z_g^2 \rangle^{1/2}$, where $\langle z_g^2 \rangle$ is defined as

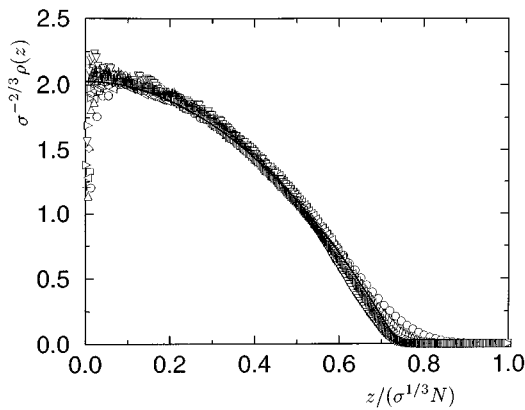


FIG. 2. Scaled monomer density profile $\sigma^{-2/3} \rho(z)$ as a function of scaled distance from the grafting surface $z / (\sigma^{1/3} N)$ of a linear brush for $(N, \sigma) = (100, 0.05)$ (circles), $(100, 0.10)$ (squares), $(100, 0.20)$ (diamonds), $(200, 0.05)$ (up triangles), $(200, 0.10)$ (left triangles), $(200, 0.20)$ (down triangles), $(400, 0.05)$ (right triangles), and $(400, 0.10)$ (crosses). The solid line corresponds to the analytical SCF result from Eq. (12).

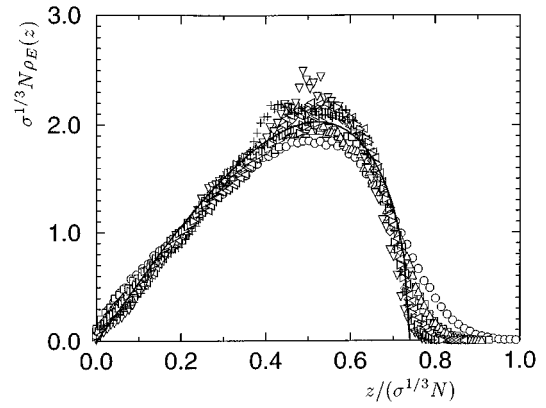


FIG. 3. Scaled chain-end probability distribution $\sigma^{1/3} N \rho_E(z)$ as a function of scaled distance from the grafting surface $z / (\sigma^{1/3} N)$ of a linear brush. The solid line corresponds to the analytical SCF result from Eq. (13). The meaning of the symbols is the same as in Fig. 2.

$$\langle z_g^2 \rangle = \frac{1}{N} \sum_{i=1}^N \left\langle \left(z_i - \frac{1}{N} \sum_{i=1}^N z_i \right)^2 \right\rangle, \quad (10)$$

are plotted in Fig. 1 as functions of $\Omega = \sigma N^{3/2}$. For convenience, in the rest of this paper we set the Kuhn length $l = 1$

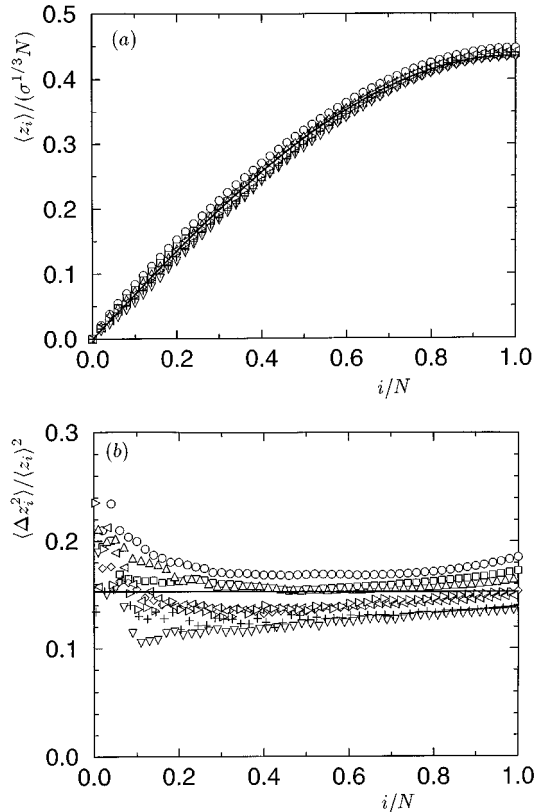


FIG. 4. (a) Scaled average brush height of monomers $\langle z_i \rangle / (\sigma^{1/3} N)$ and (b) relative z -component mean-square displacement of the monomer positions $\langle \Delta z_i^2 \rangle / \langle z_i \rangle^2$ as a function of i/N for linear chains. The solid line corresponds to the analytical SCF results from Eqs. (14) and (15). The meaning of the symbols is the same as in Fig. 2.

TABLE I. Numerical results for the conformational properties of the RBP brushes.

σ	N	$\langle z \rangle$	$\langle z_g^2 \rangle$	n_3	σ	N	$\langle z \rangle$	$\langle z_g^2 \rangle$	n_3
0.025	10	1.181	0.464	2.139	0.10	10	1.365	0.585	2.094
	20	1.816	0.933	5.015		20	2.325	1.484	4.876
	50	3.507	2.937	13.60		50	5.171	6.507	13.18
	100	6.195	8.549	27.96		100	9.865	22.60	27.06
	150	8.961	17.32	42.28		150	14.30	46.19	40.88
	200	11.59	27.86	56.65		200	19.13	81.33	54.72
	300	17.00	59.00	85.22		300	27.74	179.4	82.24
	400	22.42	101.0	113.9		400	37.53	318.7	109.6
	500	28.18	161.0	142.4		500	45.87	486.9	136.3
0.05	10	1.248	0.509	2.122	0.15	10	1.468	0.668	2.056
	20	2.008	1.125	4.969		20	2.568	1.795	4.784
	50	4.183	4.177	13.45		50	5.861	8.283	12.96
	100	7.784	13.54	27.64		100	11.25	29.18	26.59
	150	11.35	27.54	41.78		150	16.92	64.81	40.24
	200	14.77	45.90	55.87		200	22.23	113.5	53.49
	300	21.84	104.8	84.09		300	32.36	237.7	80.40
	400	29.00	181.0	112.3		400	42.65	443.4	106.9
	500	35.57	270.3	140.5		500	51.50	629.5	133.2
0.075	10	1.315	0.552	2.103	0.20	10	1.557	0.739	2.021
	20	2.175	1.313	4.915		20	2.778	2.085	4.703
	50	4.676	5.289	13.33		50	6.377	9.942	12.77
	100	8.875	17.98	27.26		100	12.36	36.98	26.15
	150	12.93	37.65	41.26		150	19.08	86.32	39.14
	200	17.10	65.16	55.29		200	24.13	139.6	52.65
	300	25.63	147.3	83.10		300	36.06	317.7	78.77
	400	33.57	249.8	110.8		400	47.05	538.3	103.9
	500	40.85	376.4	138.3		500	56.24	773.6	130.9

and the volume parameter $u=1$ since u and σ always appear as a single combination in the mean-field approximation. The figure shows an excellent agreement with the analytical SCF results: the data points fall almost exactly on the straight line characterized by a slope of $\frac{1}{3}$. The brush height h reaches an asymptotic behavior that can be approximated by

$$h = (0.74 \pm 0.02) \sigma^{1/3} N, \quad (11)$$

which is consistent with the analytical result $h = (4\sigma/\pi^2)^{1/3} N$. In Fig. 2 we show the scaling plot of the density profile $\sigma^{-2/3} \rho(z)$ as a function of $z/(\sigma^{1/3} N)$ for different surface coverages and molecular weights. The solid curve in Fig. 2 is the SCF result [7,8]

$$\sigma^{-2/3} \rho(z) = \frac{3}{2} \left[\left(\frac{\pi^2}{4} \right)^{1/3} - \left(\frac{z}{\sigma^{1/3} N} \right)^2 \right]. \quad (12)$$

The simulation results are well represented by the parabolic equation (12). The scaling dependence on N and σ of the chain-end density distribution $\rho_E(z)$ is also tested by plotting $\sigma^{1/3} N \rho_E(z)$ against $z/\sigma^{1/3} N$ in Fig. 3 together with the SCF prediction (solid curve):

$$\sigma^{1/3} N \rho_E(z) = \frac{3\pi^2}{4} \left(\frac{z}{\sigma^{1/3} N} \right) \left[\left(\frac{4}{\pi^2} \right)^{2/3} - \left(\frac{z}{\sigma^{1/3} N} \right)^2 \right]^{1/2}. \quad (13)$$

The agreement between the data points and the SCF prediction is fair; previous numerical studies [13,14] also showed that the comparison of $\rho_E(z)$ is less satisfactory. In addition, we also compared with the analytical SCF prediction the average height $\langle z_i \rangle$ of the i th monomer and the relative mean-square displacement of the monomer positions along the z axis $\langle \Delta z_i^2 \rangle / \langle z_i \rangle^2$, where $\langle \Delta z_i^2 \rangle = \langle z_i^2 \rangle - \langle z_i \rangle^2$. Once again, the data shown in Fig. 4 are well represented by the SCF theory (solid curve)

$$\frac{\langle z_i \rangle}{\sigma^{1/3} N} = \frac{3}{8} \left(\frac{\pi}{2} \right)^{1/3} \sin \frac{i\pi}{2N} \quad (14)$$

and

$$\frac{\langle \Delta z_i^2 \rangle}{\langle z_i \rangle^2} = 0.1528. \quad (15)$$

Considering the overall agreements between these numerical results and the well-known theories, we conclude that our numerical procedure provides an effective method to study the polymer brush problem.

Next, we present the numerical results for the brushes of randomly branched polymers. In order to verify the scaling equation deduced earlier in Sec. II, we examined systems with various values of σ ($=0.025, 0.05, 0.075, 0.10, 0.15, 0.20$) and N ($=10, 20, 50, 100, 150, 200, 300, 400, 500$). Table I is a

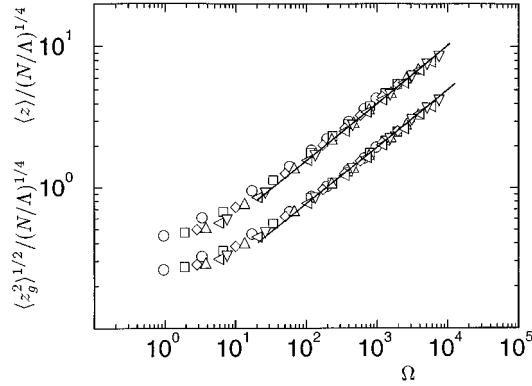


FIG. 5. Scaled average brush height $\langle z \rangle / (N/\Lambda)^{1/4}$ and the mean-square radius of gyration normal to the surface $\langle z_g^2 \rangle^{1/2} / (N/\Lambda)^{1/4}$ plotted as a function of $\Omega = \sigma N^{7/4} \Lambda^{1/4}$ on a log-log scale for $\sigma = 0.025$ (circles), 0.05 (squares), 0.075 (diamonds), 0.10 (up triangles), 0.15 (left triangles), and 0.20 (down triangles) for the brush formed by randomly branched polymers. The two straight lines indicate asymptotic behavior with the slope of 0.41.

summary of the original data obtained for the mean brush height $\langle z \rangle$, mean-square radius of gyration $\langle z_g^2 \rangle$, and the mean tribranching number n_3 from the calculations.

We show in Fig. 5 a log-log plot of $\langle z \rangle / (N/\Lambda)^{1/4}$ and $\langle z_g^2 \rangle^{1/2} / (N/\Lambda)^{1/4}$ as functions of $\Omega = \sigma N^{7/4} \Lambda^{1/4}$ for all the data points shown in Table I. It can be observed from Fig. 5 that the data for large Ω lie closely on a straight line for both $\langle z \rangle$ and $\langle z_g^2 \rangle^{1/2}$ and that the slopes of the two straight lines are almost the same. This implies that the asymptotic scaling behavior in Eq. (5) is indeed valid for large Ω . Using the data points corresponding to $\Omega \geq 20$, we estimated the brush exponent

$$\lambda = 0.41 \pm 0.02. \quad (16)$$

This value is quite close to the Flory exponent [$\lambda(\text{Flory}) = \frac{3}{7} = 0.43$] discussed above and is substantially larger than the linear-brush value [$\lambda(\text{linear}) = \frac{1}{3}$]. By examining Fig. 5, we see that the data points approach the asymptotic behavior from the above, which implies that the effective exponent determined from the numerical data is always slightly smaller than the actual value. The numerical investigation strongly supports the Flory exponent $\lambda = \frac{3}{7}$ for annealed RBP brushes.

Figures 6(a) and 6(b) show several mean density profiles $\rho(z)$ obtained for different surface coverages and molecular weights. Qualitatively, the overall shape of the mean monomer density is comparable to those found for linear polymer brushes. Because a RBP is a denser object than its linear counterparts, the density profiles are “compressed” more closely to the surface. Near the first few monomer distances from the surface, the profiles show oscillations up to about 2–3 monomer layers. Such oscillations in $\rho(z)$ were also observed in other simulations of the linear polymer brushes [10,13]. In our case, the oscillations are probably due to the discreteness of choosing a rigid bond of fixed length to connect two monomers in the model. Slightly away from the surface, the profile shows a peak. We observe that the position of the peak is insensitive to both molecular weight and

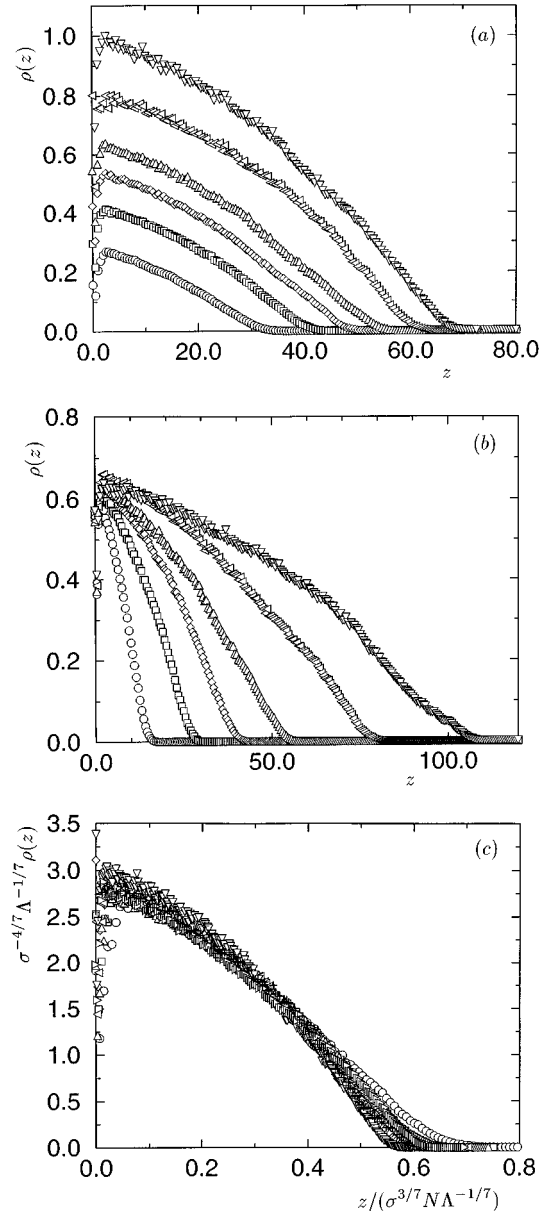


FIG. 6. Monomer density profile $\rho(z)$ as a function of distance from the grafting surface z for the brush formed by randomly branched polymers (a) corresponding to $N=200$ and $\sigma=0.025$ (circles), 0.05 (squares), 0.075 (diamonds), 0.10 (up triangles), 0.15 (left triangles), and 0.20 (down triangles); (b) corresponding to $\sigma=0.10$ and $N=50$ (circles), 100 (squares), 150 (diamonds), 200 (up triangles), 300 (left triangles), and 400 (down triangles); and (c) scaled plot for $(N, \sigma) = (100, 0.05)$ (circles), (100, 0.10) (squares), (100, 0.20) (diamonds), (200, 0.05) (up triangles), (200, 0.10) (left triangles), (200, 0.20) (down triangles), (400, 0.05) (right triangles), and (400, 0.10) (crosses).

surface coverage and that the height of the peak is independent of the molecular weight as in the case of linear chains [14]. Following the peak, the profile decays monotonically. Near the brush end, the polymers are not stretched and the monomer density decays to zero smoothly.

In order to examine the scaling behavior for RBP brushes, we plot in Fig. 6(c) the scaled profile $\sigma^{-4/7} \Lambda^{-1/7} \rho(z)$ as a function of the scaled distance $z / (\sigma^{3/7} N \Lambda^{-1/7})$ from the grafting surface for several sets of N and σ . Except near the

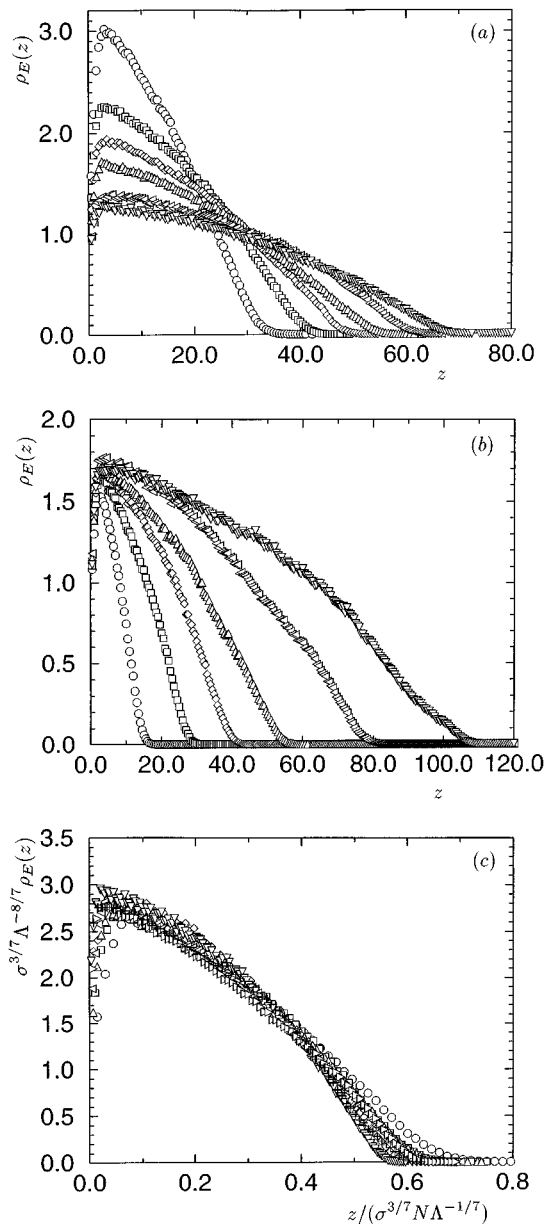


FIG. 7. Density profile of the free-end monomers $\rho_E(z)$ as a function of distance from the grafting surface z for the brush formed by randomly branched polymers. The meaning of the symbols is the same as in Fig. 6.

grafting surface and the brush end, most data collapse roughly onto a single universal curve. Note that near the brush end the decay to zero is sharper for systems of higher molecular weight or larger surface coverage. The brush height h can be estimated from the point when $\rho(z)=0$ is first approached in Fig. 6. For the larger- N limit, we have

$$h = (0.57 \pm 0.03) \sigma^{3/7} N \Lambda^{-1/7}. \quad (17)$$

The shape of the universal density profile closely resembles a parabolic curve; however, we are not able to verify analytically the existence of a parabolic function through solving the mean-field model.

We also calculated the density distributions for the free-end monomers ρ_E and for the tribranching monomers ρ_T ,

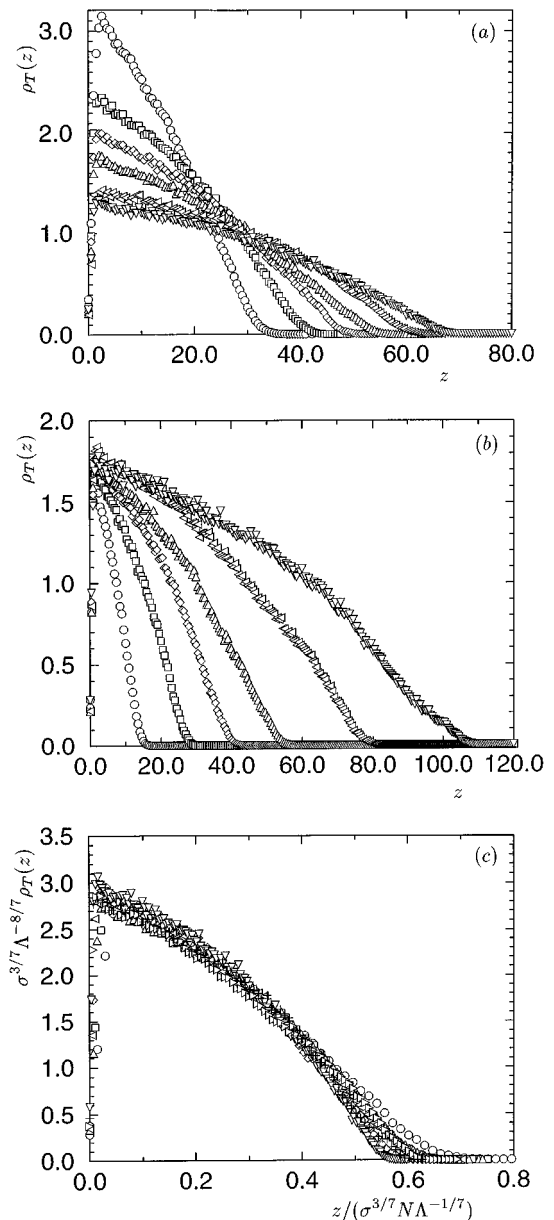


FIG. 8. Density profile of the tribranching monomers $\rho_T(z)$ as a function of distance from the grafting surface z for the brush formed by randomly branched polymers. The meaning of the symbols is the same as in Fig. 6.

which are plotted in Figs. 7 and 8. Since the branching points are randomly constructed, the profiles of $\rho_E(z)$ and $\rho_T(z)$ qualitatively display behavior similar to that of the overall monomer density profile of $\rho(z)$. These plots indicate that there is a uniform distribution of the tribranching units and the free-end units over the whole brush layer. This is very different from the chain-end density profile of linear brushes, where there is a peak (see Fig. 3) indicating that the free end will preferably stay away from the hard surface. The scaling dependence of ρ_E and ρ_T on N and σ is further demonstrated by plotting $\sigma^{3/7} \Lambda^{-8/7} \rho_E(z)$ and $\sigma^{3/7} \Lambda^{-8/7} \rho_T(z)$ against $z / \sigma^{3/7} N \Lambda^{-1/7}$ in Figs. 7(c) and 8(c) for several sets of N and σ . Again these plots show that universal asymptotic scaling behaviors exist.

V. SUMMARY

We have studied annealed RBP brushes of different molecular weights grafted on a planar surface in the good solvent condition at different values of surface coverages. We have used a single-polymer SCF approximation in which the mean field represents effectively the interactions between monomers; the mean field is expressed in terms of the local volume concentration dependence of polymers. Using an iterative Metropolis MC method for single-polymer configurations, we obtained the conformational properties numerically. We found that the average monomer height scales as $h/(N/\Lambda)^{1/4} \sim \Omega^\lambda$ for $\Omega = \sigma N^{7/4} \Lambda^{1/4} \geq 20$ for the range of parameters considered here. The “brush exponent” λ has a value of 0.41 ± 0.02 for annealed RBP brushes. The density profile is found to have the same qualitative form as that of linear-chain brushes. Most significantly, the monomer density profile also displays a parabolic-like form, which at the present has no support from an analytic solution.

Our calculation is based on the SCF approximation. It is known that such a mean-field model would fail when the spatial fluctuations of the monomer density became large. Such fluctuations become important when polymers are grafted to a surface with low surface coverage. For randomly branched polymers, the additional structural fluctuations would probably further complicate the matter. Brushes at high surface coverage are also rarely studied. Higher-order interactional terms in ρ become important; thus the mean-field potential is no longer simply proportional to the local concentration. That is another density regime where the current model fails to describe. For the moderately high coverage considered here, the mean-field theory should be adequate for capturing the main physical phenomena.

ACKNOWLEDGMENT

This work was supported by the Natural Science and Engineering Research Council of Canada.

APPENDIX: BLOB MODEL

Consider a brush formed by randomly branched polymers grafted at one end on a planar surface. We assume that they are strongly stretched along the normal to the planar surface. Schematically, grafted polymers can be subdivided into blobs of size ξ , each of them containing g monomers. Each polymer now can be regarded as a string of N/g blobs stretched along the normal to the surface, where N is the monomer number of a single polymer. Therefore, the brush height h scales as

$$h = \left(\frac{N}{g}\right) \xi. \quad (\text{A1})$$

The blob size ξ is approximately the average distance between grafted sites on the surface, which can be expressed in terms of the grafting coverage σ as

$$\xi = l \sigma^{-1/2}, \quad (\text{A2})$$

where l is the Kuhn length. The monomer number g can be obtained according to the relation given for the homogeneous system of interacting RBPs since the correlations between monomers are dominated by the excluded-volume effects within each blob. From Ref. [19], we have

$$g \sim u^{-3/7} \Lambda^{1/7} \xi^{13/7} \quad (\text{A3})$$

for a three-dimensional model, where u is the volume parameter and Λ^2 the tribranching activity [21]. Using Eqs. (A2) and (A3) in (A1) yields

$$h \sim (u \sigma)^{3/7} N \Lambda^{-1/7}, \quad (\text{A4})$$

which is the same as that obtained from the Flory-type argument, Eq. (5).

-
- [1] S. T. Milner, *Science* **251**, 905 (1991).
 [2] S. Alexander, *J. Phys. (Paris)* **38**, 983 (1977).
 [3] P. G. de Gennes, *Macromolecules* **13**, 1069 (1980).
 [4] A. K. Dolan and S. F. Edwards, *Proc. R. Soc. London Ser. A* **337**, 509 (1974); **343**, 427 (1975).
 [5] T. Cosgrove, T. Heath, B. van Lent, F. Lermakers, and J. Scheutjens, *Macromolecules* **13**, 1069 (1980).
 [6] J. M. H. M. Scheutjens and G. J. Fleer, *J. Phys. Chem.* **83**, 1619 (1979).
 [7] S. T. Milner, T. A. Witten, and M. E. Cates, *Macromolecules* **21**, 2160 (1988).
 [8] A. M. Skvortsov, A. A. Gorbunov, I. V. Pavlushkov, E. B. Zhulina, O. V. Borisov, and V. A. Priamitsyn, *Polym. Sci. USSR* **30**, 1706 (1988).
 [9] M. Muthukumar and S. Ho, *Macromolecules* **22**, 965 (1989).
 [10] M. A. Carignano and I. Szleifer, *Macromolecules* **26**, 3108 (1993).
 [11] A. Chakarabarti and R. Toral, *Macromolecules* **23**, 2016 (1990).
 [12] P. K. Lai and K. Binder, *J. Chem. Phys.* **95**, 9288 (1991).
 [13] P. K. Lai and E. B. Zhulina, *J. Phys. (France) II* **2**, 547 (1992).
 [14] M. Laradji, H. Guo, and M. J. Zuckermann, *Phys. Rev. E* **49**, 3199 (1994).
 [15] M. Murat and G. S. Grest, *Macromolecules* **22**, 4054 (1989).
 [16] M. Murat and G. S. Grest, *Phys. Rev. Lett.* **63**, 1074 (1989).
 [17] M. A. Carignano and I. Szleifer, *Macromolecules* **27**, 702 (1994).
 [18] E. B. Zhulina and T. A. Vilgis, *Macromolecules* **28**, 1008 (1995).
 [19] A. M. Gutin, A. Y. Grosberg, and E. I. Shakhnovich, *Macromolecules* **26**, 1293 (1993).
 [20] S.-M. Cui and Z. Y. Chen (unpublished).
 [21] S.-M. Cui and Z. Y. Chen, *Phys. Rev. E* **53**, 6238 (1996).
 [22] P. G. de Gennes, *Biopolymer* **6**, 715 (1968).
 [23] S.-M. Cui and Z. Y. Chen, *Phys. Rev. E* **52**, 3943 (1995).
 [24] B. H. Zimm and W. Stockmayer, *J. Chem. Phys.* **17**, 1301 (1949).